SCI. MAR., 69 (Suppl. 2): 7-15 SCIENTIA MARINA 2005

THE MAGELLAN-ANTARCTIC CONNECTION: LINKS AND FRONTIERS AT HIGH SOUTHERN LATITUDES.
*W.E. ARNTZ, G.A. LOVRICH and S. THATJE (eds.)*

# Mesoscale eddies in the Subantarctic Front - Southwest Atlantic*

PABLO D. GLORIOSO [1], ALBERTO R. PIOLA [2] and ROBERT R. LEBEN [3]

[1] British Antarctic Survey, Cambridge, UK; present address: Av. Mila Reial 113 D4, Torre en Conill, Betera, Valencia 46117, Spain. E-mail: pablo@g3golf.com
[2] Depto. Oceanografía, Servicio de Hidrografía Naval and Depto. Cs. de la Atmósfera y los Océanos, Universidad de Buenos Aires, Buenos Aires, Argentina.
[3] Colorado Center for Astrodynamics Research, University of Colorado, Boulder, USA.

SUMMARY: Satellite and ship observations in the southern southwest Atlantic (SSWA) reveal an intense eddy field and highlight the potential for using continuous real-time satellite altimetry to detect and monitor mesoscale phenomena with a view to understanding the regional circulation. The examples presented suggest that mesoscale eddies are a dominant feature of the circulation and play a fundamental role in the transport of properties along and across the Antarctic Circumpolar Current (ACC). The main ocean current in the SSWA, the Falkland-Malvinas Current (FMC), exhibits numerous embedded eddies south of 50°S which may contribute to the patchiness, transport and mixing of passive scalars by this strong, turbulent current. Large eddies associated with meanders are observed in the ACC fronts, some of them remaining stationary for long periods. Two particular cases are examined using a satellite altimeter in combination with in situ observations, suggesting that cross-frontal eddy transport and strong meandering occur where the ACC flow intensifies along the sub-Antarctic Front (SAF) and the Southern ACC Front (SACCF).

*Keywords*: southwest Atlantic, mesoscale, eddies, transport, Falkland-Malvinas Current.

RESUMEN: EDDIES DE MESOESCALA EN EL FRENTE SUBANTÁRTICO, ATLÁNTICO SUDOESTE. – Observaciones *in situ* y satelitales en el sudoeste del Océano Atlántico Sur revelan un intenso campo de eddies e indican la utilidad de la altimetría satelital para detectar, monitorear y mejorar la compresión de fenómenos de mesoescala en la región. Los ejemplos presentados sugieren que los eddies de mesoescala son una característica dominante de la circulación y juegan un papel fundamental en el transporte de propiedades a lo largo y a través de la Corriente Circumpolar Antártica (CCA). Al sur de 50°S la principal corriente en esta región, la Corriente de Malvinas exhibe numerosos eddies, los que pueden contribuir al patrón de manchas, y al transporte y la mezcla de trazadores pasivos de esta intensa y turbulenta corriente. En los frentes de la CCA se observan grandes eddies asociados con meandros, algunos de estos eddies permanecen estacionarios durante largos períodos de tiempo. Se analizan dos casos particulares empleando altimetría satelital en combinación con observaciones *in situ* que sugieren que donde la CCA se intensifica, a lo largo del Frente Subantártico y el Frente Sur de la CCA, se producen intensos transportes a través de la corriente y fuertes meandramientos.

*Palabras clave*: Atlántico suroccidental, mesoescala, eddies, transporte, Corriente de Falkland/Malvinas.

## INTRODUCTION

The view of ocean currents as smooth, streamlined flows in geostrophic balance has been replaced by the modern view of the ocean as a turbulent fluid. Remote sensing and satellite-tracked drifting buoys have reinforced this view by resolving the broadband temporal and spatial variability associated with turbulent scales of motion (Stammer, 1997). Mesoscale turbulence arising from baroclinic and barotropic instability, wind forcing and topographic interactions influence the variability of ocean cur-

*Received January 1, 2004. Accepted June 21, 2005.

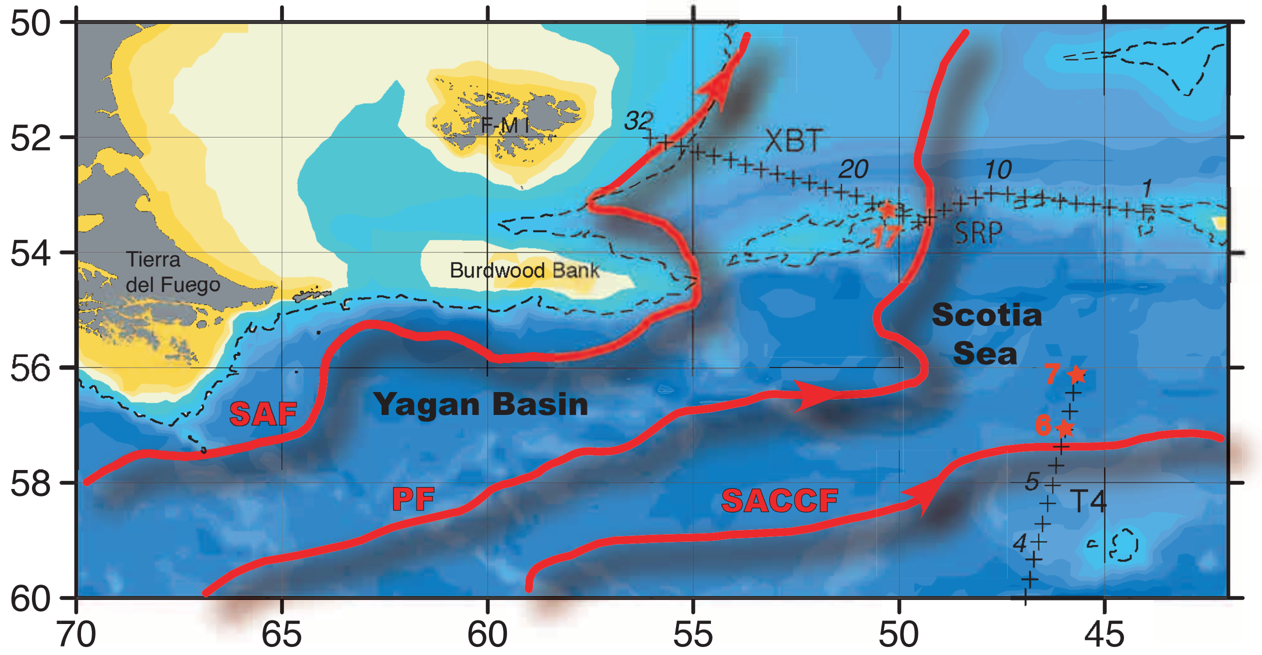


FIG. 1. – Topographic map of the southern southwest Atlantic (SSWA) depicting the Shag Rocks Passage (SRP). The red lines indicate the mean position of the sub-Antarctic Front (SAF), the Polar Front (PF) and the Southern Antarctic Circumpolar Current Front (SACCF) as described in Orsi *et al.*, 1995). The XBT transect consisted of 32 launches and was carried out on 21-22 Feb 2003. Transect T4 consisted of CTD casts and XBT launches. XBT 17 and CTDs 6 and 7 in T4 are indicated by the red stars. The dashed line is the 1500 m isobath.

rents and generate eddies, fronts and jets, which are significant contributors in the transport of properties such as heat, momentum and nutrients.

Mesoscale processes also have a large influence on the development and diversity of biological species at different trophic levels, from phytoplankton blooms to the life cycle of whales (Davis *et al.*, 2002). For instance, according to recent findings (Thatje and Fuentes, 2003), planktonic larvae from South America may have reached Antarctic waters by an intrusion of Subantarctic warm-water rings across the ACC fronts. Moreover, mesoscale phenomena are crucial to our understanding of ocean circulation and climate change, and to a large extent may determine the location and variability of fisheries. Here we present evidence that mesoscale turbulence in the SSWA may play a substantial role in the transport of properties within and across major currents of the ACC system, such as the Falkland-Malvinas Current (FMC). This evidence comes from observations at sea and from remote sensing.

The main ocean current in the SSWA (Fig. 1) is the FMC, a cold stream linked to the Subantarctic Front. To place the FMC in context, it carries about 40 to 70 Sv (1 Sv = $1 \times 10^6$ $m^3$ $s^{-1}$, Peterson, 1992; Vivier and Provost, 1999), or 200 times the outflow of the Amazon River, and in concert with the Patagonian shelf tides, it constitutes the dominant oceanographic signal in the SW South Atlantic, which is a distinct biogeochemical province (Longhurst, 1995). The FMC originates in the northern Drake Passage as a branch of the ACC associated with the SAF, and then flows northward, around the Burdwood Bank, steered by the edge of the Patagonian shelf (Piola and Gordon, 1989).

Further south, the ACC tends to be concentrated in frontal jets steered by the bottom topography (Nowlin *et al.*, 1977; Pollard *et al.*, 2002). The input of eastward momentum by the wind stress that generates the ACC is transferred vertically to the deep ocean, where it is dissipated by bottom friction, and hence the system is dynamically balanced (see Gent *et al.*, 2001 and references therein). This transfer of momentum is possible due to the generation of transient and standing eddies caused by the presence of topographic barriers in the path of the ACC, and is a form of interfacial stress set up by the eddies (McWilliams *et al.*, 1978; Wolff *et al.*, 1991).

Satellite altimetry shows that the SSWA is a region of enhanced eddy activity east of the Drake Passage (Gille *et al.,* 2000), where eddies might be generated by topographic features partially blocking the ACC (Wolff *et al.*, 1991). The continental shelf extending south from Tierra del Fuego, submarine ridges and seamounts are probably inducing the relatively high surface eddy kinetic energy observed downstream of Drake Passage in the northwest Scotia Sea.

This paper addresses the need to characterise mesoscale eddies in the SSWA, given their significant influence in the regional circulation and their potential for the transport of properties. We present examples that indicate agreement between remote sensing and in situ observations, and point out the potential of using continuous real-time satellite altimetry for detecting, monitoring and improving our understanding of mesoscale phenomena in a remote region that is beyond the present coverage of microwave-derived sea surface temperature and is often covered by clouds, which obscure visible and infrared imagery.

## OBSERVATIONS

Extraordinary evidence of complex mesoscale patterns in the SSWA comes from images taken by SeaWiFS (Sea-viewing Wide Field-of-view Sensor). The example shown in Figure 2 illustrates complex non-linear patterns of stretching and folding of streaklines evolving around eddies and dipole vortices, indicating that eddies indeed play a significant part in the dynamics of the FMC. The FMC itself is visible as a lighter band of colour along the shelf slope to the east of the Falkland-Malvinas Islands. Note the counter-clockwise eddy of the same colour that appears to have detached from the current and drifted to the east. Notably, north of about 50ºS the

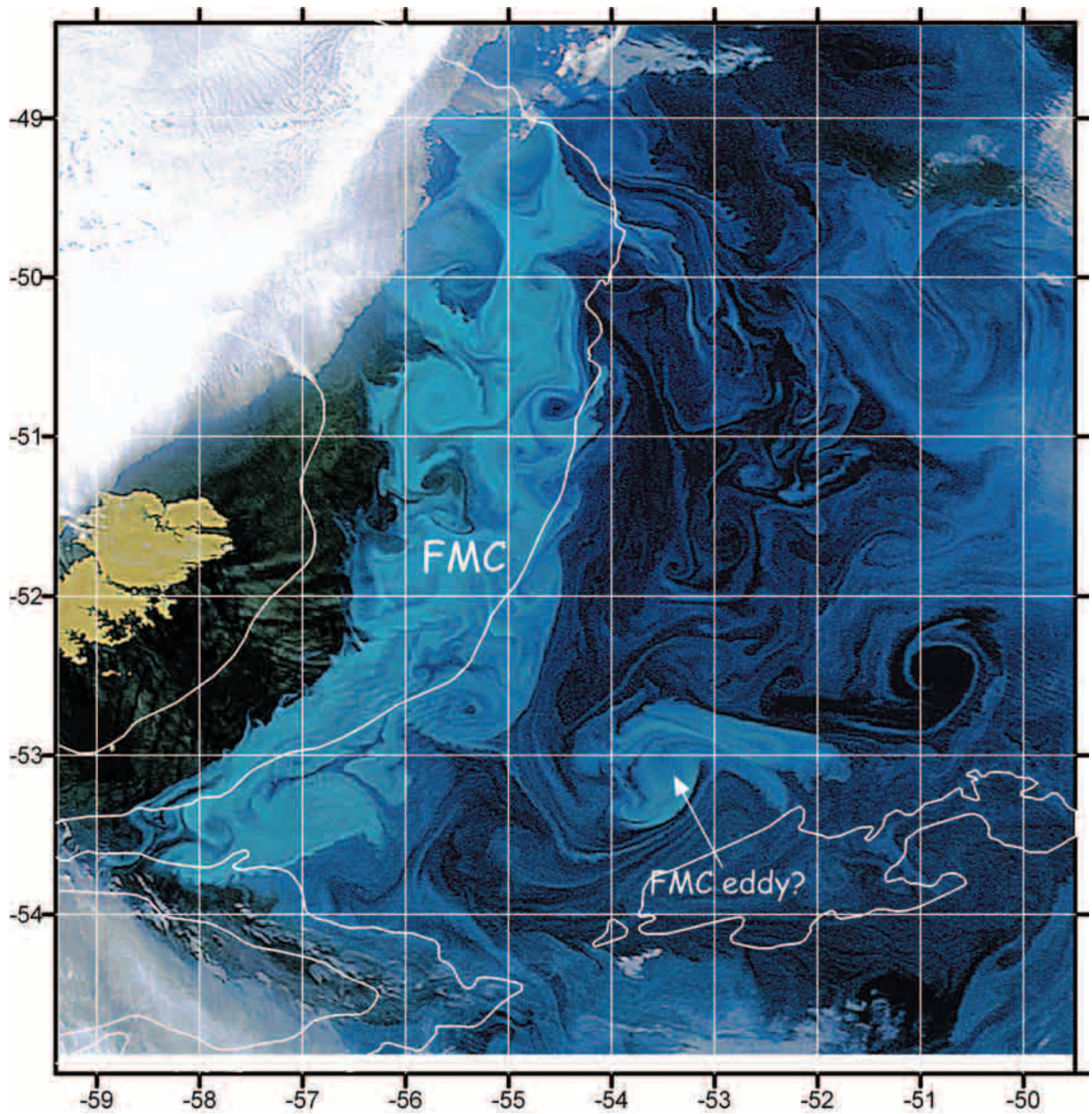


FIG. 2. – SeaWiFS true-colour image for 11 Nov 2001 of the Falkland-Malvinas Current (FMC), which flows along the shelf edge, offshore from the Falkland-Malvinas Islands. The abundance of eddies is highlighted by the presence of phytoplankton. White areas on the top- and bottom-left of the image are clouds. The white contours are the 200 m and 1500 m isobaths. Image provided by the SeaWiFS Project, NASA/Goddard Space Flight Center, and Orbimage.

FMC appears as a very low eddy energy region (Goni and Wainer, 2001), suggesting that the current stabilises downstream, presumably as it is steered by the steep bottom topography along the western edge of the Argentine Basin.

CTD (Conductivity-Temperature-Depth) data collected by the Fisheries Department of the Falkland Islands on a crisscross grid across the FMC in July 1999 gave a first indication of the presence of eddies embedded in the current (Glorioso, 2002). The extent of these eddies down into the water column has been described by performing a water mass analysis using the Optimum Multi-Parameter (OMP) method (Tomczak, 1981). The results obtained from this analysis have indicated that the observed FMC eddies reached the full water depth (more than 1000 m) and upwelled deep water to the surface layer of the ocean. Thus, the FMC eddies may play a significant role in the vertical redistribution of properties, supplying nutrients and other substances to the upper ocean.

Figure 3 presents expendable bathythermograph (XBT) data taken on 21-22 Feb 2003 at 32 positions every 15 nm, along a transect (see location in Fig. 1) that was designed to sample the underlying structure of eddies detected in satellite altimetry maps. In this figure, the relatively warm Antarctic Intermediate Water (AAIW) close to the continental shelf to the west is in sharp contrast with the colder Circumpolar Deep Water (CDW, carried by the ACC) to the east. Both water masses appear below a warmer surface layer due to seasonal heating.

This XBT section gives a fairly synoptic view of the eddies that were encountered. Eddy locations were monitored with sea surface height (SSH) anomaly fields produced by blending altimeter data from, for example, the TOPEX/Poseidon and ERS-2 satellites (Leben *et al.*, 2002) to accurately map the ocean mesoscale variability. Satellite altimeters measure changes in SSH due to the redistribution of the water column integrated mass and changes in water density, i.e. the barotropic and baroclinic components.

XBT positions 9 to 15 covered the Shag Rocks Passage (SRP in Fig. 1), transecting the mean path of the Polar Front (PF). In the vertical temperature

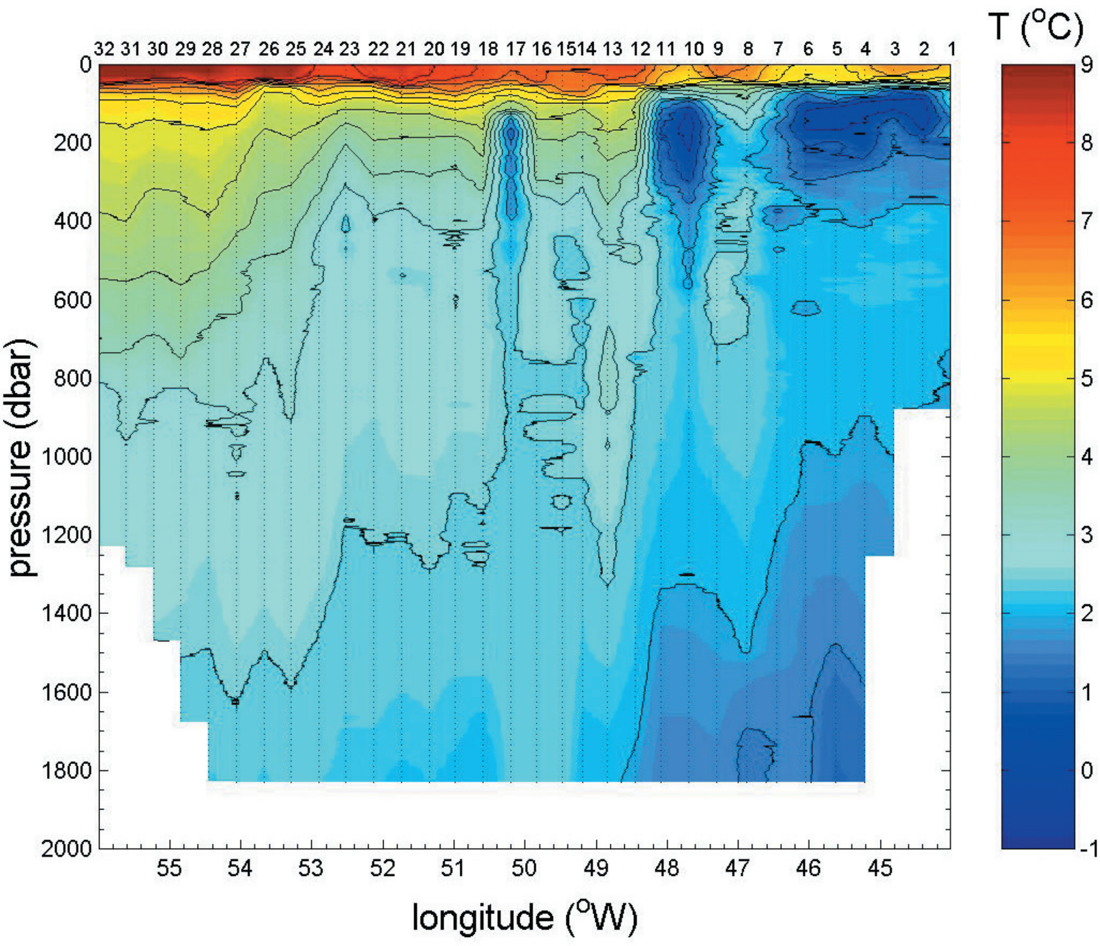


FIG. 3. – XBT temperature section (see location in Fig. 1 and text for details).

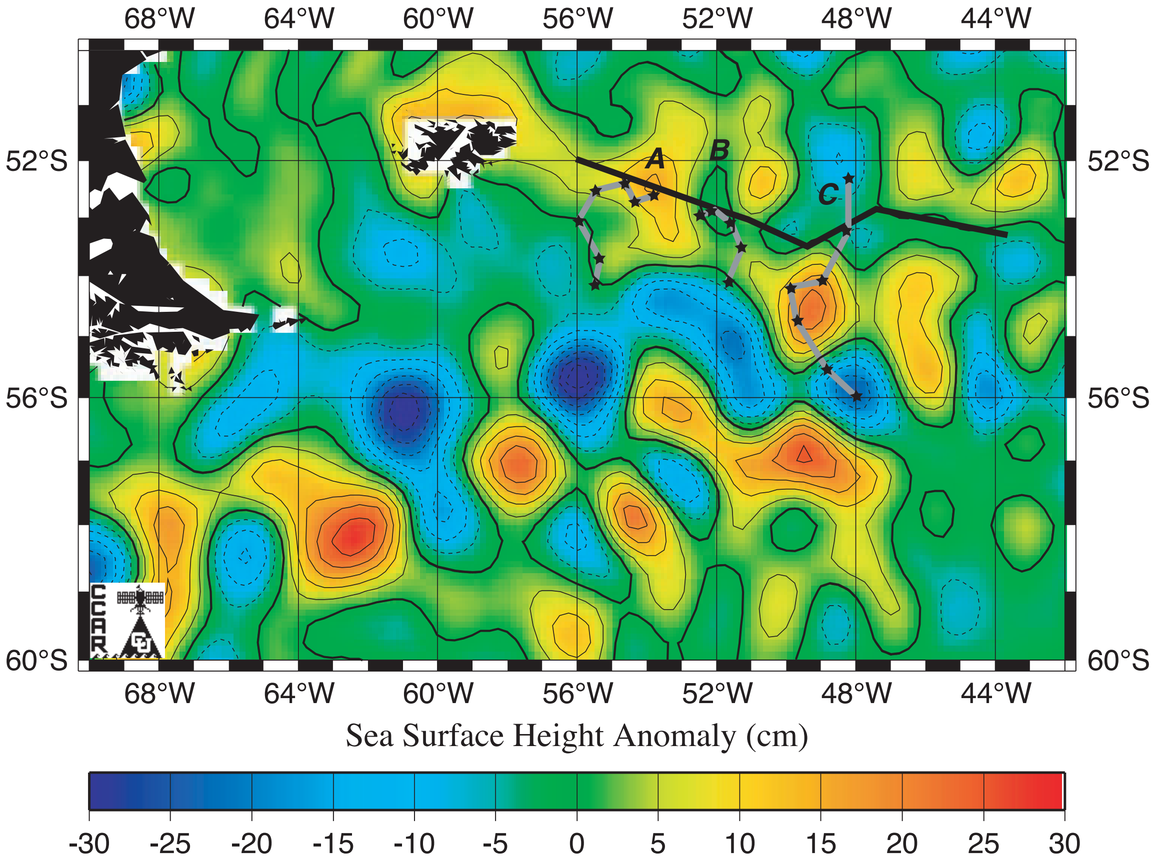


FIG. 4. – TOPEX/JASON/ERS-2/GFO altimetry analysis map for 22 Feb 2003 showing clockwise (anticlockwise) eddies with lower (higher) sea surface height (SSH) anomaly in blue (red). The heavy contour is the zero SSH anomaly. The XBT transect is indicated in the figure by the black line. Eddies labelled A, B and C are referred to in the text and their tracks, from 01 December 2002 to 12 March 2003, are depicted by the gray lines (black stars indicate where the eddies were clearly identified) as they moved north.

section (Fig. 3), the PF is seen as the strong horizontal gradient between XBTs 11 and 12, shallower than 400 m. Further west, the isotherms slope downward from XBTs 23 to 25, particularly at depth, suggesting the location here of the ACC jet associated with the SAF, whose mean position (see Fig. 1) would locate it closer to position 31. XBT 17 is located over the North Scotia Ridge, about 40 km west of the Shag Rock Passage, where the ACC jet associated with the Polar Front permeates through the ridge (Fig. 1). The 3 °C isotherm rises from about 450 m at XBT 18 to <150 m at XBT 17, but the thermocline located at about 80 m depth is nearly flat, and there is no surface signature of this eddy (Fig. 3). The vertical structure of low temperature centred at XBT 17, with a minimum of < 1.5 °C located at about 200 m depth, suggests that this cold eddy may have been shed from the PF, as it interacts with the bottom topography. This temperature distribution is similar to that found further north along 51°S (Arhan *et al.*, 2002).

The upward sloping of isotherms around XBT 23 associated with lower sea surface temperature (SST) similarly to the eddy observed at XBT 17, is interpreted as a clockwise rotating eddy, whose evolution was followed in a sequence of altimetry maps similar to the one shown in Figure 4. The mesoscale SSH anomaly map of 22 February 2003 shown in Figure 4 was constructed by blending Topex/POSEIDON and Jason data within ± 10 days with ERS and Geosat follow-on (GFO) data within ± 17 days. These "hindcast" maps depict the mesoscale eddy field for retrospective studies better than the "nowcast" maps produced in near real-time that only use along-track data collected before the analysis date. Both hindcast and nowcast maps are based on along-track data that have been high-pass filtered to retain mesoscale wavelengths, as described in Leben *et al.* (2002). The location of the XBT transect is indicated on this map, as well as the track of three eddies (A, B and C). These tracks start from the south on 01 Dec 2002 and end on 12 Mar 2003 following a general northerly direction. The black marks on the tracks indicate where these eddies were clearly identified throughout this period, even though their signature changed with time, perhaps due to changes in

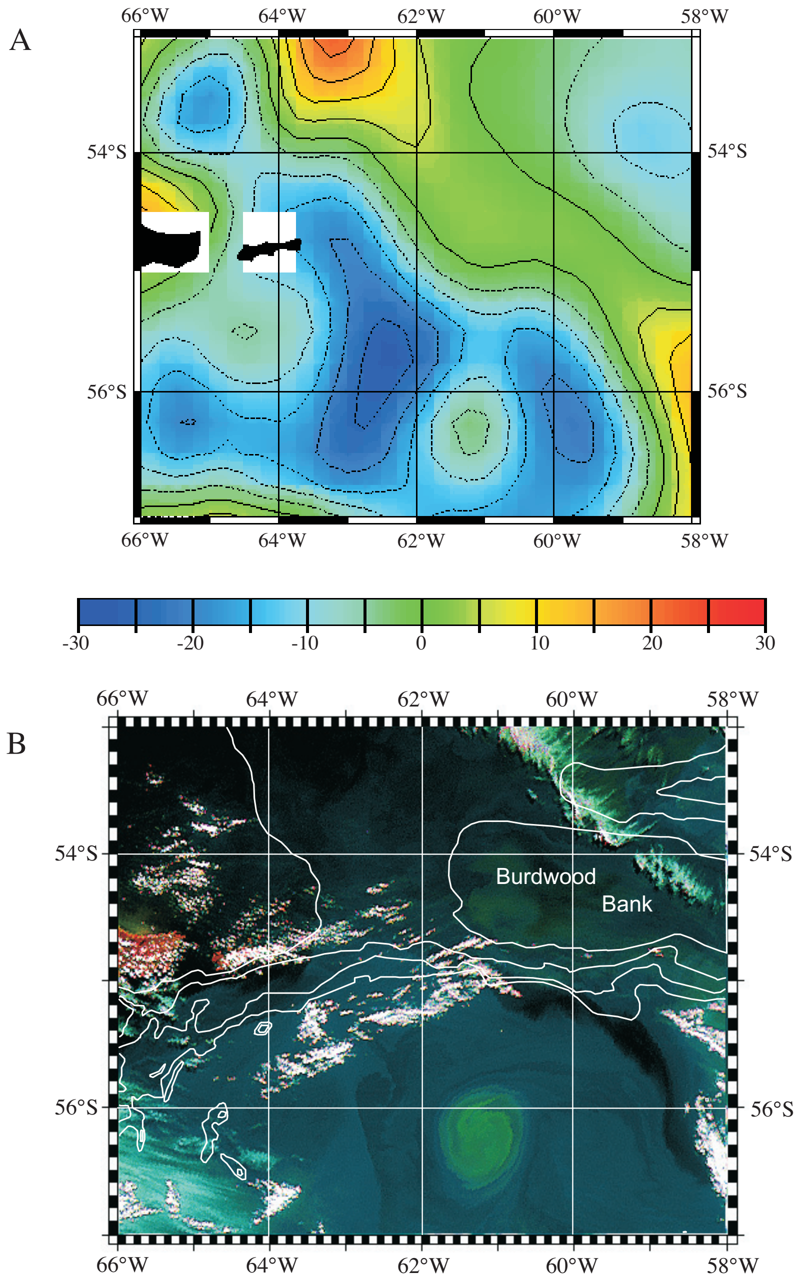


FIG. 5. – (A) TOPEX/ERS-2 altimetry analysis map and (B) enhanced true-colour SeaWiFS image (provided by the SeaWiFS Project, NASA/Goddard Space Flight Centre, and Orbimage) for 04 Mar 1998. The white contours in B are the 200, 1000, 2000 and 3000 m isobaths.

their strength and/or variations in sampling associated with the altimeter coverage. The sequence of altimetry maps (not shown here) indicated, for instance, that the eddy in the middle (B), which appears in Figure 4 with its centre of lower SSH anomaly at 52°W and 53°S, was stationary at that location for about two months. The relatively intense, small-scale eddy at XBT 17 (Fig. 3), which presumably detached from the Polar Front Zone, is also apparent in Figure 4 at 50°W, 53°S.

Further south, the eddy field revealed by the sea surface height anomaly maps is substantially more intense, with surface signatures greater than 30 cm. These large eddies found east of the Drake Passage might be generated by the partial blocking of the ACC by the tip of the continental shelf south of Tierra del Fuego. This hydrodynamic generation mechanism would agree with numerical experiments (Wolff *et al.*, 1991). After being generated, these major eddies interact with each other and follow a

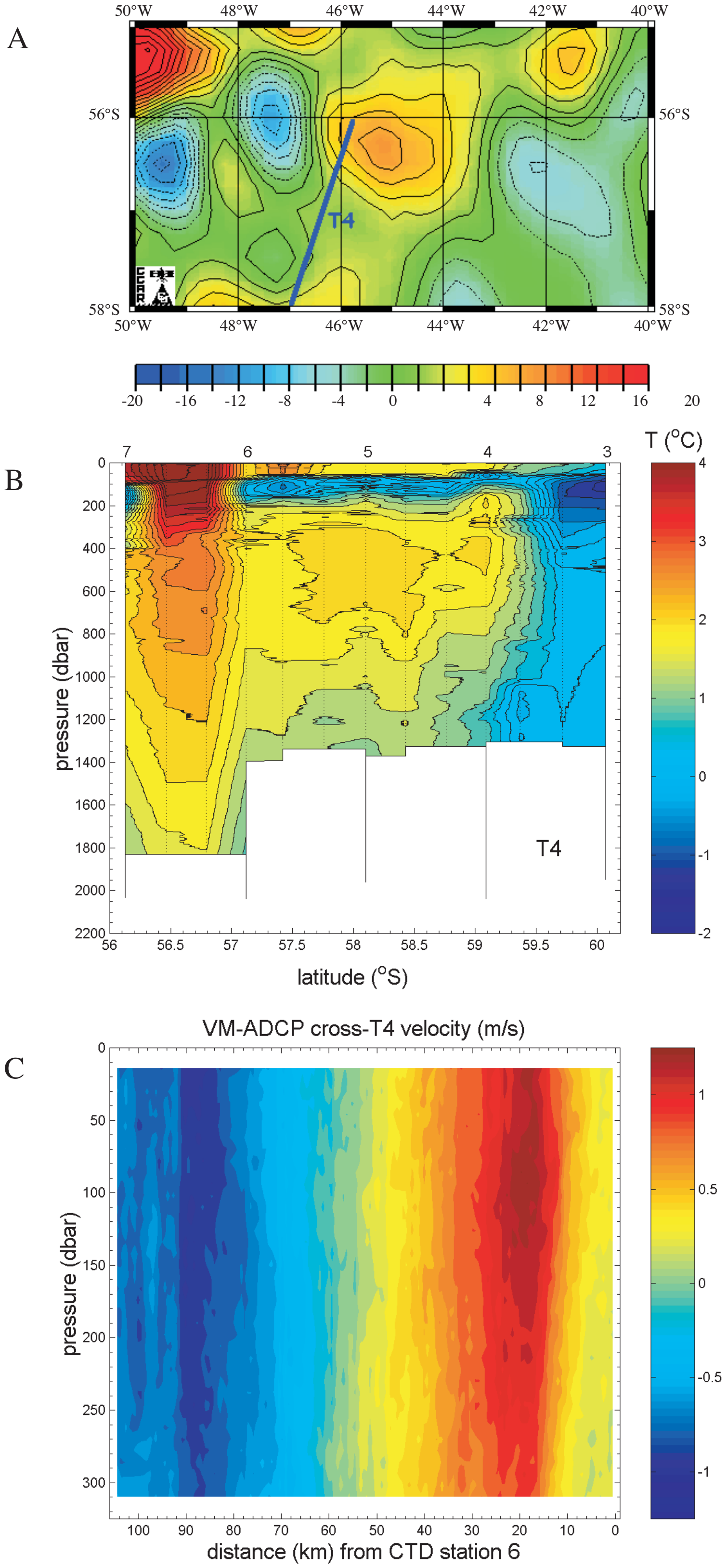


FIG. 6. – (A) Altimetry map for 24 Jan 2003, where T4 indicates the section surveyed by the RRS *James Clark Ross* referred to in the text. (B) Vertical distribution of temperature along T4, where numbers along the sea surface indicate CTD stations and dashed vertical lines indicate XBT launches. (C) Contours of horizontal velocity across T4, between CTD stations 6 and 7, measured by the vessel-mounted ADCP plotted as a function of distance to CTD 6. Positive eastward (red) and negative westward (blue) velocities indicate the anticlockwise rotation of the eddy.

general path towards the NE. However, they are nearly stationary for several weeks, allowing jet flows concentrated between the counter-rotating adjacent eddies to produce strong meridional and westward (i.e. against the ACC) currents. Measurements taken during repeated transects at the Drake Passage and spectral analysis of SSH anomaly TOPEX data indicate that these large eddies have time scales of about 40 days and spatial scales of between 150 and 200 km (Sprintall *et al.*, 1997, and subsequent work by these authors).

A combination of altimetry and SeaWiFS satellite data (Fig. 5) provides evidence of the evolution of another kind of eddy, which was formed on the continental slope and may have entrained water from the Patagonia shelf to the south, across the SAF and into the Yagan Basin. The feature has a radius of about 40 km and shows a positive SSH anomaly of the order of 20 cm relative to the surrounding waters. There is remarkable correspondence between the two remote sensing data products, in terms of the location, size and sense of rotation of this eddy, while the SeaWiFS image indicates that it contains higher phytoplankton biomass than the surrounding water.

Even though these anticlockwise Yagan eddies do not appear to be very common in an examined four-year time series (1999 to 2002) of altimetry maps, their occurrence might be significant to the transfer of properties across the shelf edge and the SAF. Because the southern Patagonia shelf shows the peak of biological production in February (Longhurst, 1998), this eddy may be advecting shelf organisms into the Yagan Basin. In addition, the eddy dynamics may act to further enhance the biological activity locally, for instance by upwelling nutrient-rich Subantarctic Zone waters into the photic layer. In this particular case, this eddy travelled south and back to the north, across isobaths, after reaching as far south as its position shown in Figure 5.

A similar example was detected in late January 2003 further east, at about the same latitude. This is shown in Figure 6a, where the larger eddy that appears in the centre of this altimetry map has higher SSH anomaly and therefore rotates anticlockwise. The eddy radius as determined from the altimetry is about 95 km and the SSH anomaly is 25 cm higher at the centre than around the edges. The blue line depicts the end section of transect T4, which was part of a survey by the RRS *James Clark Ross* that crisscrossed the Scotia Sea in the austral summer of 2003. Data from this transect are used here to characterise this eddy.

Figure 6b is the vertical section of temperature corresponding to transect T4, where numbers along the sea surface indicate CTD stations (3 to 7) in between which two XBT probes were launched (locations indicated by the vertical dashed lines). This temperature distribution shows the contrast between relatively warmer water associated with the ACC and colder water from the Weddell Sea. A subsurface temperature minimum ($T < 0°C$) located at 120-150 m depth is observed everywhere in T4, except between CTD stations 6 and 7, suggesting that the SACCF is located north of station 7, and of its mean climatological position (see Fig. 1 and Orsi *et al.*, 1995). The temperature maximum between stations 6 and 7, extending from the sea surface to beyond 1800 m, characterises the vertical structure of the eddy, which may have been generated by a sharp meander in the SACCF and drifted south. Note that the subsurface temperature minimum ($< 1°C$) near 150 m is interrupted by the eddy. Previous work described comparable cases with the aid of SST satellite images (García *et al.*, 2002; Meredith *at al.*, 2003).

The vessel-mounted RDI acoustic Doppler current profiler (ADCP) provided another source of data to characterise this energetic warm-core eddy. Figure 6c shows the cross-transect component of the velocity, where positive and negative values indicate eastward and westward flow respectively, between CTD stations 6 and 7. Despite the limited reach of the ADCP to about 300 m of depth, the anticlockwise rotation of the eddy is clearly seen. Rotational velocities are nil at the eddy core and rise beyond 1m $s^{-1}$ at about 35 km from the centre, where the hydrographic section shows the largest horizontal temperature gradients. The rotational speed of the eastward flowing branch, shown in red, rapidly decreases to ~ 0.8 m $s^{-1}$ at 400 m, in accordance with the decreasing horizontal temperature gradient with depth (Fig. 6b).

## CONCLUSIONS

There is ample evidence that eddies are widespread phenomena in the southern southwest Atlantic. This comes from SeaWiFS colour images of the ocean surface, where phytoplankton acts as a tracer that displays a wide range of mesoscale structures, and also from maps produced by blending

TOPEX, Jason, ERS-2 and GFO altimetry data, an invaluable means of detecting and monitoring eddies and their associated currents in near-real-time, particularly for a remote region like the SSWA that is often covered by clouds and is located beyond the present coverage of microwave-derived sea surface temperature.

The most plausible mechanism involved in the generation of eddies in the SSWA is the partial blocking of the ACC by submarine topographic features, which would generate highly barotropic standing and transient eddies and eddy dipoles (Wolff *et al.*, 1991) similar to those we have observed. It is also possible that the amplification of instabilities, perhaps responding to atmospheric forcing, into sharp meandering and eddy spin-off from the ACC fronts east of the Drake Passage, may result in a cross-frontal exchange of water properties. In the Yagan Basin, continental slope eddies are likely to mix water properties between shelf and oceanic environments, moving across bathymetry as has been observed in the Gulf of Mexico (Ohlmann *et al.*, 2001), or to export water masses away from regions where they were generated.

The examples presented show that there is agreement between the sea surface signature of eddies in the SSH anomaly maps and the vertical structure revealed by the XBT and CTD measurements, and also between altimetry maps and SeaWiFS imagery. The evidence shown improves our understanding and encourages the use of altimeter data in future research of mesoscale eddies in the SSWA.

## ACKNOWLEDGEMENTS

ARP acknowledges the support from the Inter-American Institute for Global Change Research grant CRN-61. RRL acknowledges the support provided by NASA contract 1238953.

## REFERENCES

Arhan, M., A.C. Naveira Garabato, K.J. Heywood and D.P. Stevens. – 2002. The Antarctic Circumpolar Current between the Falkland Islands and South Georgia. *J. Phys. Oceanogr.*, 32: 1914-1931.

Davis, R.W., J.G. Ortega-Ortiz, C.A. Ribic, W.E. Evans, D.C. Biggs, P.H. Ressler, R.B. Cady, R.R. Leben, K.D. Mullin and B. Würsig. – 2002. Cetacean habitat in the northern Gulf of Mexico. *Deep- Sea Res. I*, 49: 121-142.

García, M.A., I. Bladé, A. Cruzado, Z. Velásquez, H. García, J. Puigdefàbregas and J. Sospreda. – 2002. Observed variability of water properties and transports on the World Ocean Circulation Experiment SR1b section across the Antarctic Circumpolar Current. *J. Geophys. Res.,* 107: 3162-3181.

Gent, P.R., W.G. Large and F.O. Bryan. – 2001. What sets the mean transport through Drake Passage? *J. Geophys. Res.*, 106: 2693-2712.

Gille, S.T., M.M. Yale and D.T. Sandwell. – 2000. Global correlation of mesoscale ocean variability with seafloor roughness from satellite altimetry. *Geophys. Res. Lett.*, 27: 1251-1254.

Glorioso, P.D. – 2002. Modeling the southwest Atlantic. *Aquatic conservation: marine and freshwater ecosystems*, 12: 27-37.

Goni, G.J. and I. Wainer. – 2001. Investigation of the Brazil Current front variability from altimeter data. *J. Geophys. Res.,* 106: 31117-31128.

Leben, R.R., G.H. Born and B.R. Engebreth. – 2002. Operational altimeter data processing for mesoscale monitoring. *Marine Geodesy*, 25: 3-18.

Longhurst, A. – 1995. Seasonal cycles of pelagic production and consumption. *Progr. Oceanogr.*, 36: 77-167.

Longhurst, A. – 1998. *Ecological geography of the sea*. Academic Press, San Diego.

McWilliams, J.C., W.H. Holland and J.H.S. Chow. – 1978. A description of numerical Antarctic circumpolar currents. *Dyn. Atmos. Oceans,* 2: 213-291.

Meredith, M.P., J.L. Watkins, E.J. Murphy, P. Ward, D.G. Bone, S.E. Thorpe, S.A. Grant and R.S. Ladkin. – 2003. Southern ACC front to the northeast of South Georgia: Pathways, characteristics, and fluxes. *J. Geophys. Res.,* 108: 3162-3178.

Nowlin W.D. Jr., T. Whitworth III, and R.D. Pillsbury. – 1977. Structure and transport of the Antarctic Circumpolar Current at Drake Passage from short-term measurements. *J. Phys. Oceanogr.*, 7: 788-802.

Ohlmann, J.C., P.P. Niiler, C.A. Fox and R.R. Leben. – 2001. Eddy energy and shelf interactions in the Gulf of Mexico. *J. Geophys. Res.*, 106: 2605-2620.

Orsi, A.H., T. Whitworth III, and W.D. Nowlin Jr. – 1995. On the meridional extent and fronts of the Antarctic Circumpolar Current. *Deep-Sea Res.*, 42: 641-673.

Peterson, R.G. – 1992. The boundary current in the western Argentine Basin. *Deep-Sea Res.*, Part A, 39: 623-644.

Piola, A.R. and A.L. Gordon. – 1989. Intermediate waters of the western South Atlantic. *Deep-Sea Res.*, 36: 1-16.

Pollard, R.T., M.I. Lucas and J.F. Read. – 2002. Physical controls on biogeochemical zonation in the Southern Ocean. *Deep-Sea Res. II*, 49: 3289-3305.

Sprintall, J., R. Peterson, D. Roemmich and J. Gallo. – 1997. High resolution XBT/XCTD measurements across Drake Passage. *International WOCE Newsletter*, 29: 18-19.

Stammer, D. – 1997. Global characteristics of ocean variability estimated from regional TOPEX/POSEIDON altimeter measurements. *J. Phys. Oceanogr.,* 27: 1743-1769.

Thatje, S. and V. Fuentes. – 2003. First record of anomuran and brachyuran larvae (Crustacea: Decapoda) from Antarctic waters. *Polar Biol.*, 26: 279-282.

Tomczak, M. – 1981. A multiparameter extension of temperature/salinity diagram techniques for the analysis of non-isopycnal mixing. *Progr. Oceanogr.*, 10: 147-171.

Viver, F. and C. Provost. – 1999. Volume transport of the Malvinas Current: Can the flow be monitored by TOPEX/POSEIDON? *J. Geophys. Res.,* 108: 21105-21122.

Wolff, J.O., E. Maier-Reimer and D.J. Olbers. – 1991. Wind-driven flow over topography in a zonal b-plane channel: a quasi-geostrophic model of the Antarctic Circumpolar Current. *J. Phys. Oceanogr.*, 21: 236-264.